A NEW ART CODE FOR TOMOGRAPHIC INTERFEROMETRY

H. Tan and D. Modarress
Spectron Development Laboratories Inc.
3303 Harbor Blvd., Suite G-3
Costa Mesa, California 92626

ABSTRACT

A new ART code based on the iterative refinement method of least squares solution for tomographic reconstruction is presented. Accuracy and the convergence of the technique is evaluated through the application of numerically generated interferometric data. It was found that, in general, the accuracy of the results were superior to other reported techniques. The iterative method unconditionally converged to a solution for which the residual was minimum. The effects of increased input data error, limited total viewing angle, and reduced number of input data were studied. The inversion error was found to be only a function of the input data error. The convergence rate, on the other hand, was affected by all three parameters. Finally, the technique was applied to experimental data and results reported.

Key Words: Tomography, Interferometry, holography, image reconstruction

I. INTRODUCTION

During recent years, image reconstruction techniques have been successfully applied to several fields such as medicine, astronomy, electron microscopy, nuclear magnetic resonance, geophysics and optical interferometry. An extensive review can be found in Reference 1.

In 1964, prior to the development of optical holography the axially symmetric density field had been reconstructed by using the inversion of Abel's integral equation[2]. Under symmetry conditions the Radon transform reduces to the Abel equation. Since 1965, holographic interferometry has been applied to aerodynamics, heat transfer and combustion problems. These developments are discussed in detail by Vest[3].

There are several difficulties associated with the reconstruction of phase objects:

(a) No sharp boundaries can be defined for phase objects. The definition of the reconstruction region is based on a priori information about the flow field. In general, the contribution of the phase object outside the reconstruction zone is assumed to be negligible.

(b) Relatively large errors are present in the interferometry data. The optical path differences are recorded as interference fringes. The accuracy of the fringe data ordinarily may not be better than 1/2 of the fringe spacing. In

addition, for an unsymmetric density field, the number of fringes for each projection varies for different view angles resulting in a nonuniform data set. The ideal projection data is a set of non-overlapping, equally spaced, parallel rays covering the whole reconstruction region.

(c) Only the relative phase shift of the projection can be measured by the interferogram data. There is, therefore, a possibility of incorrect identification of fringe numbers. This results in a set of "slightly" inconsistent data.

The mathematical reconstruction method employed in such cases should not be overly sensitive to the "noisy" or inconsistant data.

Although the Radon transformation

$$\ell(p,\theta) = \int_{-\infty}^{+\infty}\int n(x,y)\delta\left[p - x\cos(\theta) - y\sin(\theta)\right]dxdy \qquad (1)$$

provides a rigorous solution to the problem of reconstruction from projections, the solution is uniquely determined only by an infinite set of perfect projections. Here, ℓ is the optical path length, n is the refractive index, δ is the Dirac delta function, θ is the projection angle, p is the coordinate along the projection plane, and x and y are the coordinates describing the reconstruction region. In practical problems, the discrete nature of projection data and the unavoidable measurement errors may result in the failure of reconstruction.

In this paper, the iterative refinement method of least squares solution for tomographic interferometry is discussed. A complete set of computer codes for density reconstruction from holographic interferograms was made. The effects of projection number, limited viewing angle and the measurement error on the reconstructed image are determined through numerical experimentation. The flow field around the tip region of a revolving helicopter rotor blade was reconstructed from 40 interferograms. The results of the reconstructed density field are presented.

II. ITERATIVE REFINEMENT METHOD OF LEAST SQUARE SOLUTION

In principle, the ART (algebraic reconstruction technique) algorithms are the schemes for solving a large system of linear equations. The reconstruction region is divided into a square grid (M = m x m cell) and the refractive index within each cell or pixel, n_{ij}, is assumed constant. The Radon transformation then reduces to a set of discrete linear equations

$$\sum_{i=1}^{m} \sum_{j=1}^{m} W_{ij}(p,\Theta)\, n_{ij} = L(p,\Theta) \qquad (2)$$

where $W_{ij}(p,\theta)$ are weight factors determined from geometric relations. It should be noted that only those factors associated with pixels through which the projection ray passes are nonzero. For k different

projection angles, each having n nonoverlapping and equally spaced parallel rays, the number of equations N, is given by N = k x n.

Equation (2) can be written in the form

$$C\,X + L = 0 \tag{3}$$

where, L and X are N and M dimensional vectors respectively, and C is the coefficient matrix with N X M elements. Equation (3) can be transformed into a symmetric, positive definite, NORMAL EQUATION given by

$$C^T L + C^T C\,X = 0 \tag{4}$$

In practice, due to measurement errors and other inconsistencies, Equation (3) becomes

$$R = C\,X + L \tag{5}$$

where R is the residual vector. An approximate solution is sought for which the Euclidean norm of the residual vector $\|R\|$ is minimum. The Euclidean norm is defined as $\|R\| = \sqrt{\sum_i R_i \cdot R_i^*}$. The solution of the normal equation gives the standard least square solution of (3).

Procedures for obtaining solutions to a large system of linear equations can be found in a number of different scientific areas. Iterative techniques have been widely used. It begins with an initial estimate and then it repeatedly modifies the estimate until some threshold condition is satisfied. There are different ways to modify the

estimate. The effectiveness of a method depends on the matrix character. Considering the features of matrix C (large and sparse) and relatively large measurement errors, the method of CONJUGATE GRADIANTS is found to be applicable for image reconstruction.[4]

The computer procedures of conjugate gradiant method are as follows:

Initial vector

$$k = 0: \quad X(0) = 0; \; R(0) = L \tag{6}$$

For iterative number k = 1,2...

$$r(k-1) = C^T R(k-1) \tag{7}$$

$$s(k) = - r(k-1) \text{ for } k = 1$$

$$s(k) = - r(k-1) + s(k-1)\|r(k-1)\|/\|r(k-2)\| \text{ for } k > 1 \tag{8}$$

$$q(k) = C\, s(k) \tag{9}$$

$$X(k) = X(k-1) + s(k)\|r(k-1)\|/\|q(k)\| \tag{10}$$

$$R(k) = R(k-1) + q(k)\|r(k-1)\|/\|q(k)\| \tag{11}$$

The matrix C has only five percent nonzero elements. It can be stored permanently or, in the case of limited storage capacity, may be computed according to a simple geometric relation for every ray. The vectors that must be stored are X, R, s, and q. Accordingly, a procedure written in PASCAL running under CPM-86 with MT+86 compiler has been written. This procedure runs on IBM PC microcomputer, and is limited to 20 x 20 mesh size.

It can be proven[5] that: The norm of the residual vector R decreases with increasing iteration number. Thus, in principle, this code is a technique minimizing the residual R to the level determined by the inherent errors associated with the computer truncation and measurement data. Therefore, the final reconstruction accuracy is determined by data noise. Here the errors associated with the measurement of the optical path length (fringe lines) are the major attributor to the data noise.

To evaluate the characteristics of the developed tomography code, a numerically generated density field, Figure 1a, was used as the input for the numerical test. It represents the calculated air density distribution over the tip region of the rotor blade in a plane above the blade [6]. The distribution of the refractive index variance, $x = (n_o - n)$, is calculated and shown in Figure 1b. The data for the integral optical length difference as a function of ray parameters, θ and p, was generated from Equation (2). The errors associated with optical length measurement, encountered in real tomography, were artificially added to the fringe data file. Fringe round-off errors of ± 0.5, ± 0.05 and ± 0.005 were used here. The reconstruction code was parametrically evaluated for different numbers of equations and total viewing angles. The numerical test matrix is shown in Table 1.

Figure 2 shows the reconstructed field for Case 1 after different iterations. The overall features are apparent after two iterations and further refinement of the solution is obtained with additional iterations. The total reconstructed error, R_r, is also noted on Figure 2. Here, the reconstruction error is defined as

$$R_r = \sqrt{\sum_i \sum_j \left[x_{ij,in} - x_{ij,rec}\right]^2 / \sum_i \sum_j \left[x_{ij,in}\right]^2} \qquad (12)$$

where $x_{ij,in}$, and $x_{ij,rec}$ are input and reconstructed refractive index variances, respectively.

The dependence of the residual vector norm on the number of iterations for Cases 1 to 7 of Table 1 is shown on Figure 3. Figures 4, 5 and 6 demonstrate the effects of fringe number round-off error and view angle range on the reconstruction error. From these and other numerical experimentations, the following conclusion may be drawn:

- The convergence rate is increased as the projection ray number, N, is increased. The corresponding inversion error for a sufficient number of iterations is, in general, independent of N.

- The normal of the residual vector, R, in all cases, unconditionally converges to a limit which is a strong function of the input data error. The resulting error for the first few iterations is independent of the input data error. However, for more accurate input data, additional iterations result in more accurate results. This underlines the importance of the accuracy of the data set. It also proposes a guideline for determining the maximum number of iterations based on the rate of change of the residual.

Finally, limited look angles, (>30°) do not have a significant effect on the convergence rate or the accuracy of the reconstructed data. Acceptable results were obtained for a total view angle of 30°. Care must be taken to ensure that sufficient information is recorded on the interferograms when the view angle limitations are imposed.

III. THE PROCEDURE FOR PROCESSING EXPERIMENTAL DATA

Figure 7 shows the holographic interferometry arrangement at the AVRADCOM Laboratory of NASA Ames for studying the flow around a revolving helicopter blade.[7] The coordinate system (x,y) is wing-fixed (x-spanwise, y-chordwise). The projection of point "A" on the wing defines the origin for coordinate p along any azimuthal angle. The photograph of a typical interferogram is shown in Figure 8.

Forty interferograms were digitized using a Tektronix 4112 display terminal and a graphic tablet. The data were reduced and a map of the optical path as a function of height above the blade was developed. Data at each elevation and for all viewing angles were grouped (Z-files), and constituted the input data for the reconstruction code.

The reconstructed density distribution, (ρ/ρ_o), produced by the tomographic reconstruction code is shown in Figures 9 & 10 for the heights z = 0.5, 1, 1.5 and 2 inches (chord C = 3 inches; the leading edge of the blade Y/C = -0.5; aspect ratio = 13.7). The optimum number of iterations was about 3 to 6 for the experimental data. The computation time on an IBM PC was approximately 3 minutes per iteration.

IV. DISCUSSION

A new ART code based on the iterative refinement method of least square solution is developed for tomographic reconstruction of the three-dimensional density field. The features of the technique was investigated using numerically generated interferometry data. It is shown that, in general, the ART code used here, is capable of reconstructing phase objects using limited viewing angle or using data with relatively large errors.

In comparison to other reconstruction techniques, it is believed that it is possible to obtain more accurate results with the ART code.

For similar numerical tests, the reconstructed mean-square error for view angles of ±90° and ±40° were reported to be 6.7% and 11%, respectively, when the convolution back projections technique was used.(6) The corresponding values for R_r become 26% and 33%, respectively. Similar situations were examined in Cases 3 and 10 with R_r at only 3% and 10% for 20 iterations. On the other hand, the computation time for iterative techniques are generally higher than some other techniques.

An important feature of the technique is that with limited resolution (say, 20 x 20), it is possible to repeatedly use the same code and zoom into the regions surrounding important features of the flow, and hence, reconstruct the flow field in greater detail. For this, the input data for the subsequent analysis must be corrected.

Finally, a strong feature of the reconstruction code is its ability to accept data within limited view angles. The density field of the

numerically generated data was reconstructed for a total view angle of 30° and with a final error of 10%. This result is extremely important when the application of tomography to the flow field within a wind tunnel is considered.

ACKNOWLEDGEMENTS

The work described herein was supported by the U.S. Army Research Office under Contract No. DAAG29-83-C-0012.

REFERENCES

1. Deans, S. R., The Radon Transform and Some of its Applications, Chap.1, Wiley, New York (1983).
2. Barakat, R., J. Math and Phys., Cambridge Mass., 43,325 (1964).
3. Vest, C. M., Holographic Interferometry, Wiley, New York (1979).
4. Reid, J. K., Large Sparse Sets of Linear Equations, edited by J. K. Reid, Academic Press (1971).
5. Westlake, J. R., Handbook of Numerical Inversion and Solution of Linear Equations, Wiley, New York (1968).
6. Snyder, R. and Hesselink, L., Applied Optics, 23(20),3650 (1984).
7. Kittleson, J. K. and Yu, Y., AIAA 23rd Aerospace Sciences Meeting, Jan 14-17, Reno, Nevada (1985).

TABLE 1. THE NUMERICAL TEST MATRIX

CASE	FRINGE NUMBER ROUND OFF ERROR	VIEW ANGLE (degree)	NUMBER OF VIEWS	NUMBER OF POINTS PER VIEW
1	0.005	0 .. 180	61	20
2	0.005	0 .. 90	61	20
3	0.005	0 .. 180	31	20
4	0.050	0 .. 180	61	20
5	0.050	0 .. 180	31	20
6	0.500	0 .. 180	61	20
7	0.500	0 .. 180	31	20
8	0.005	-75 .. 75	31	20
9	0.005	-60 .. 60	31	20
10	0.005	-45 .. 45	31	20
11	0.005	-30 .. 30	31	20
12	0.005	-15 .. 15	31	20
13	0.050	-75 .. 75	31	20
14	0.050	-60 .. 60	31	20
15	0.050	-45 .. 45	31	20
16	0.050	-30 .. 30	31	20
17	0.050	-15 .. 15	31	20

LIST OF FIGURES

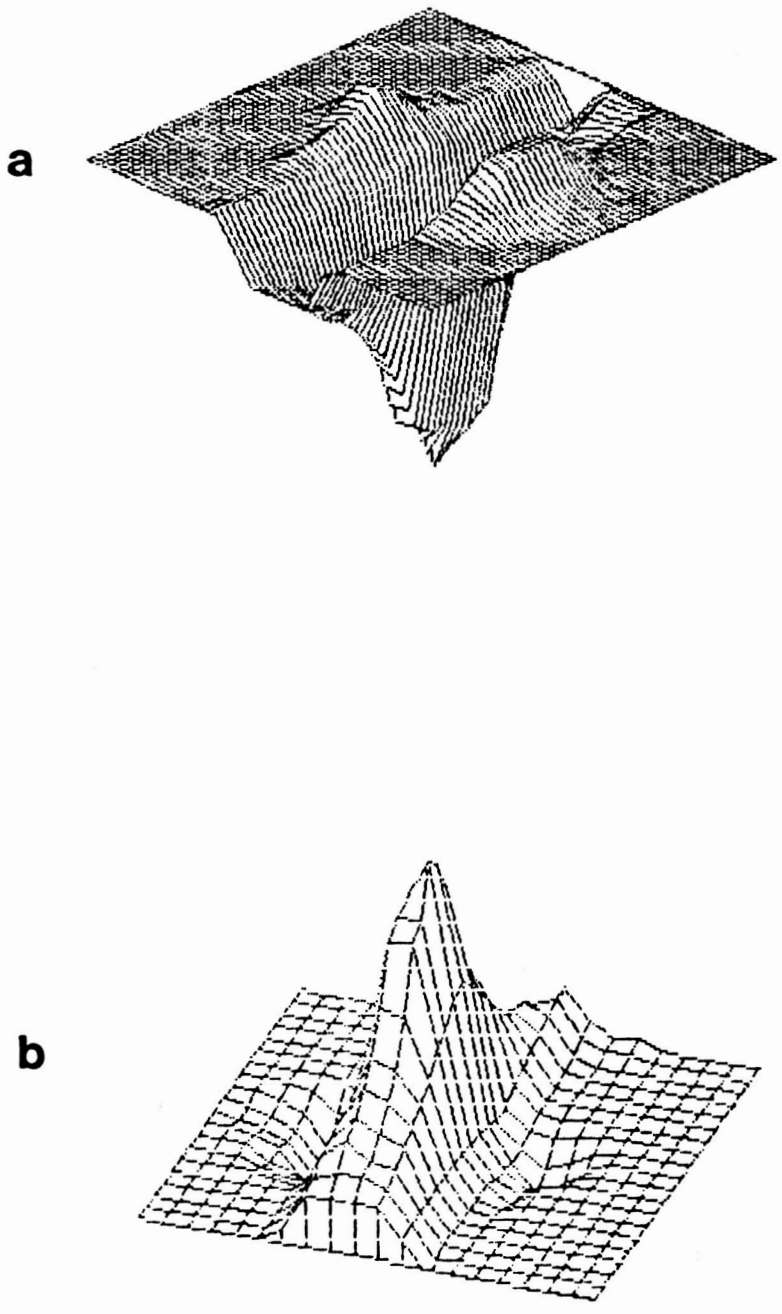

Figure 1. Numerically generated density and refractive index distribution.

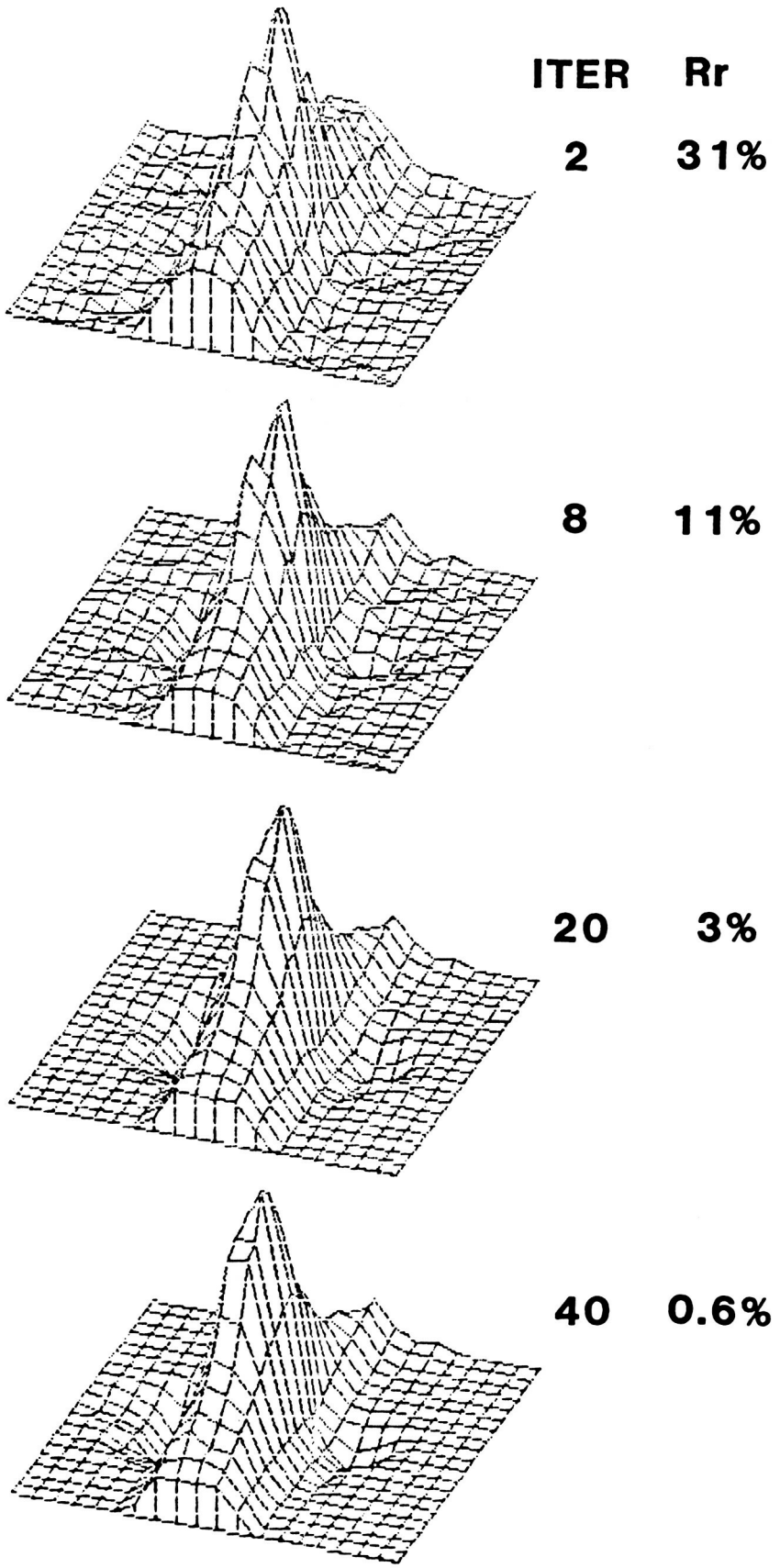

Figure 2. Reconstructed field of refractive index variance (n_o-n) for Case 1.

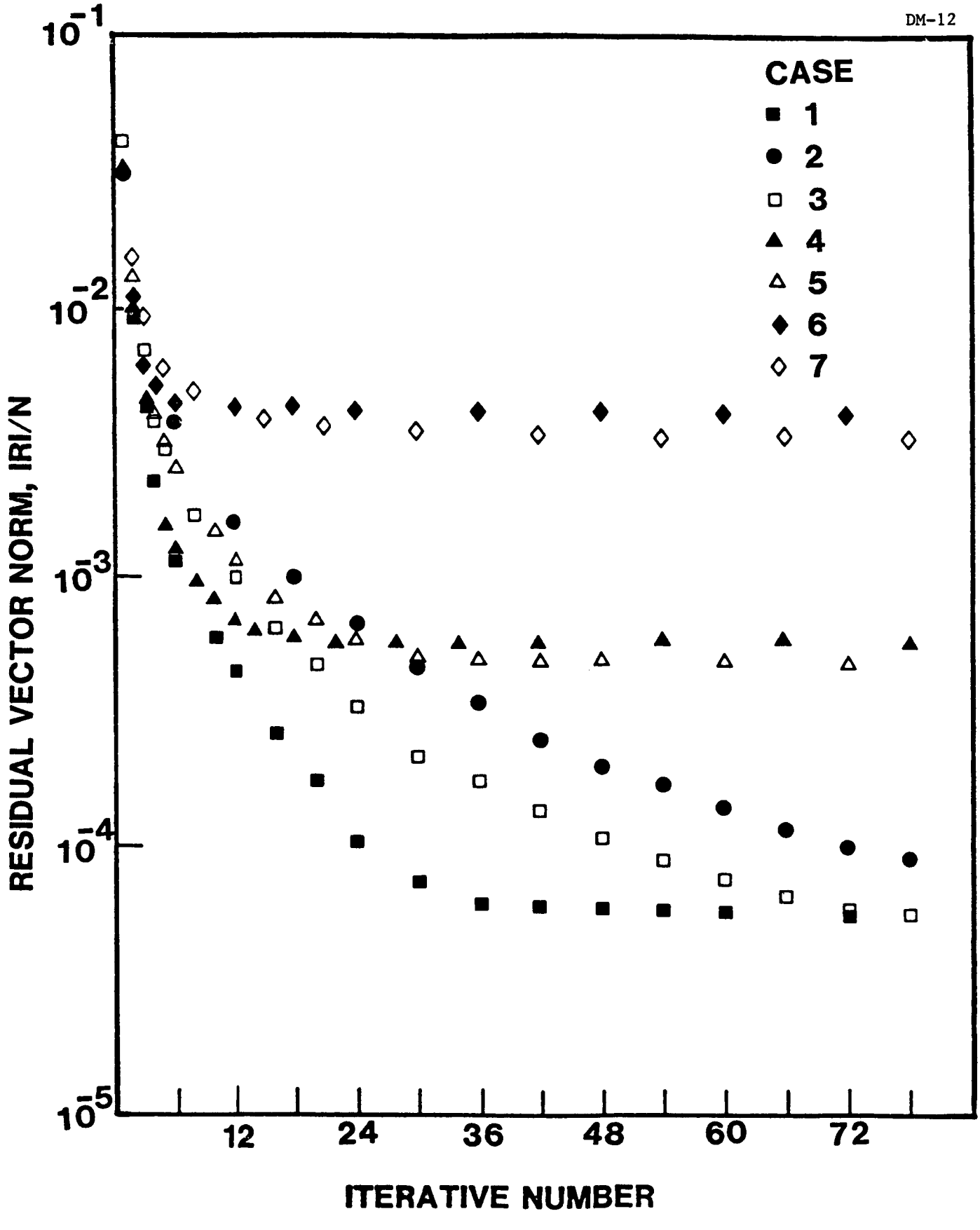

Figure 3. Residual vector norm vs. iterative number for Cases 1-7.

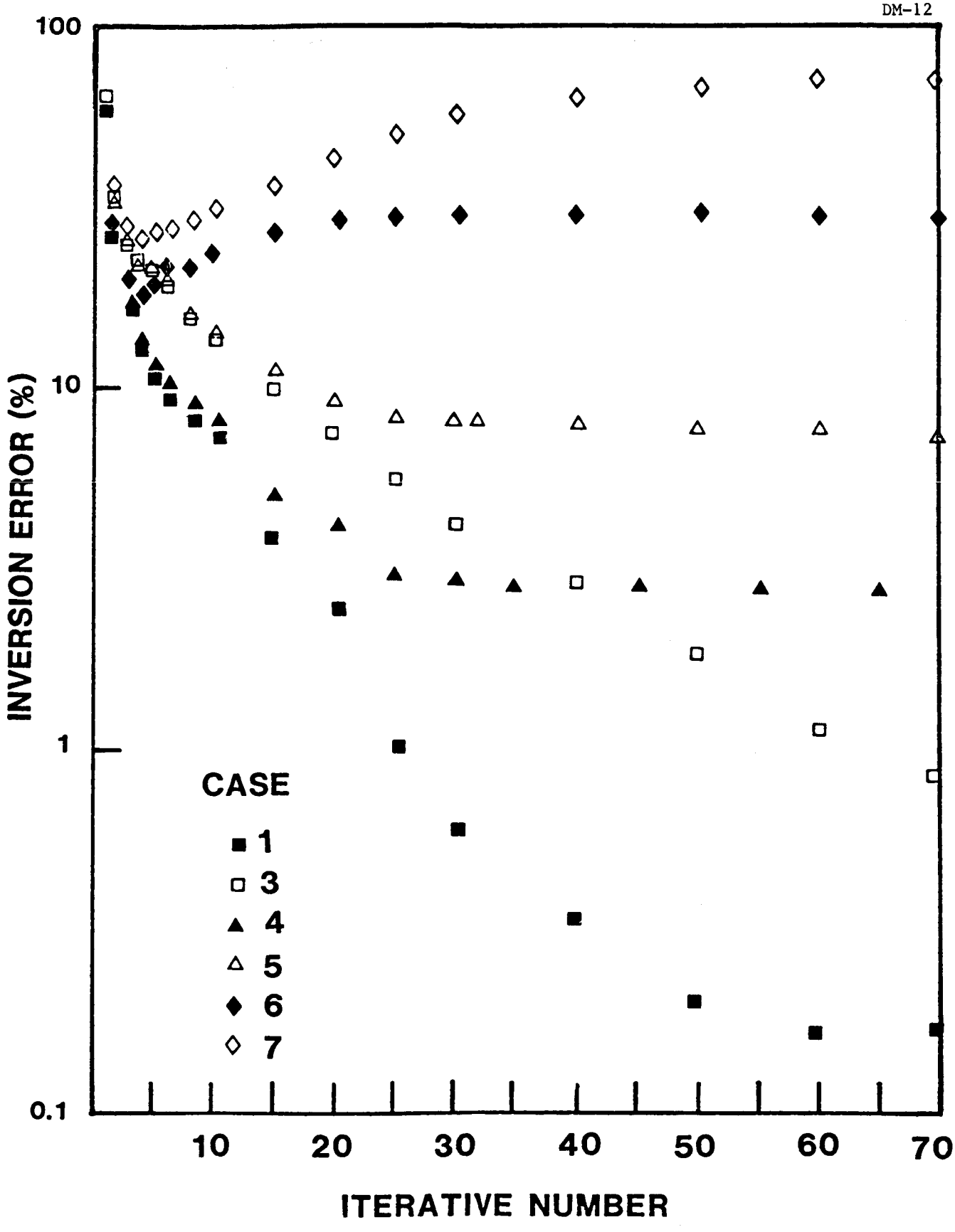

Figure 4. Inversion errors vs. iterative number for Cases 1-7.

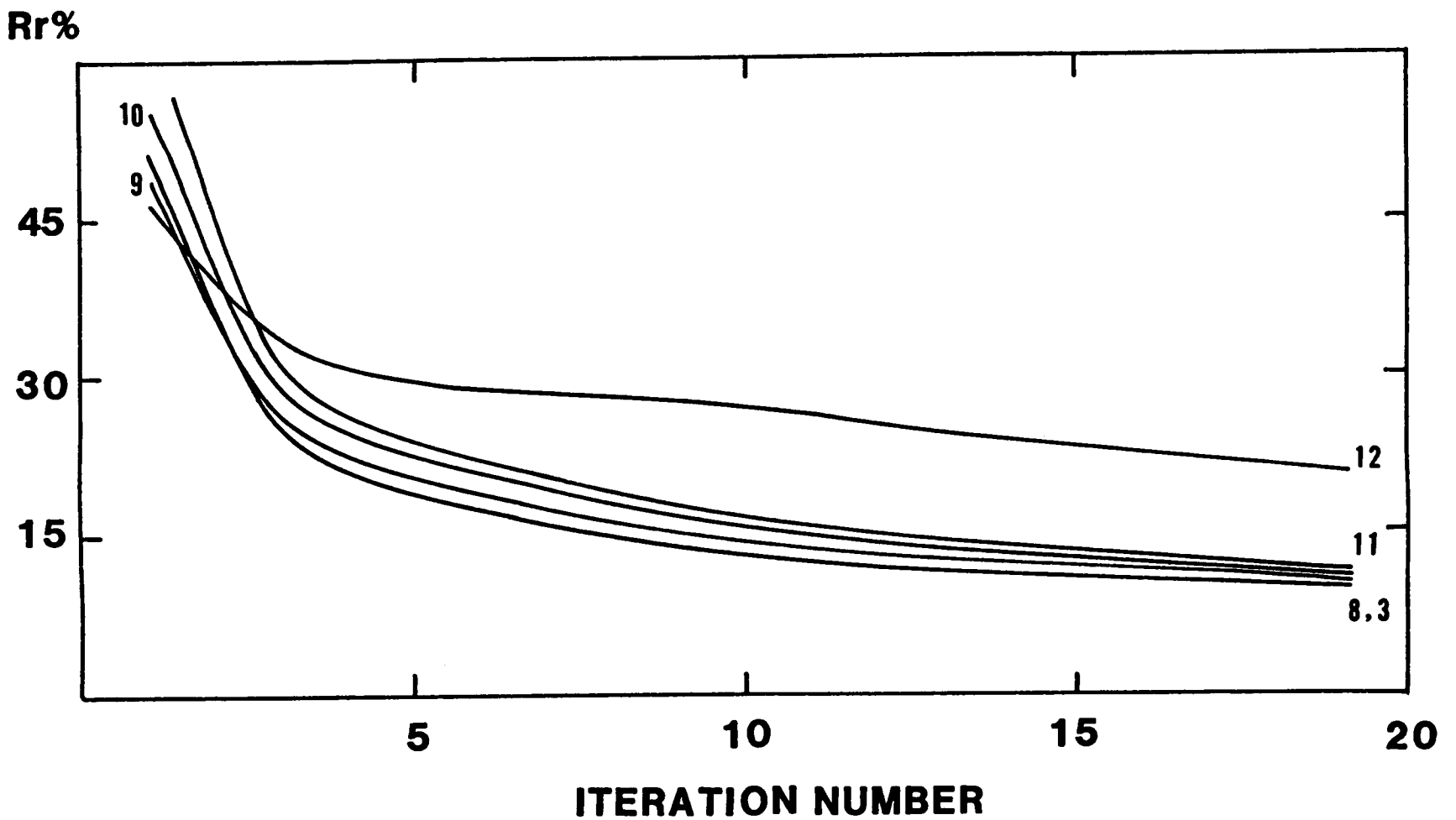

Figure 5. Inversion errors vs. iteration number for different view angles (fringe number round-off error = 0.005 λ).

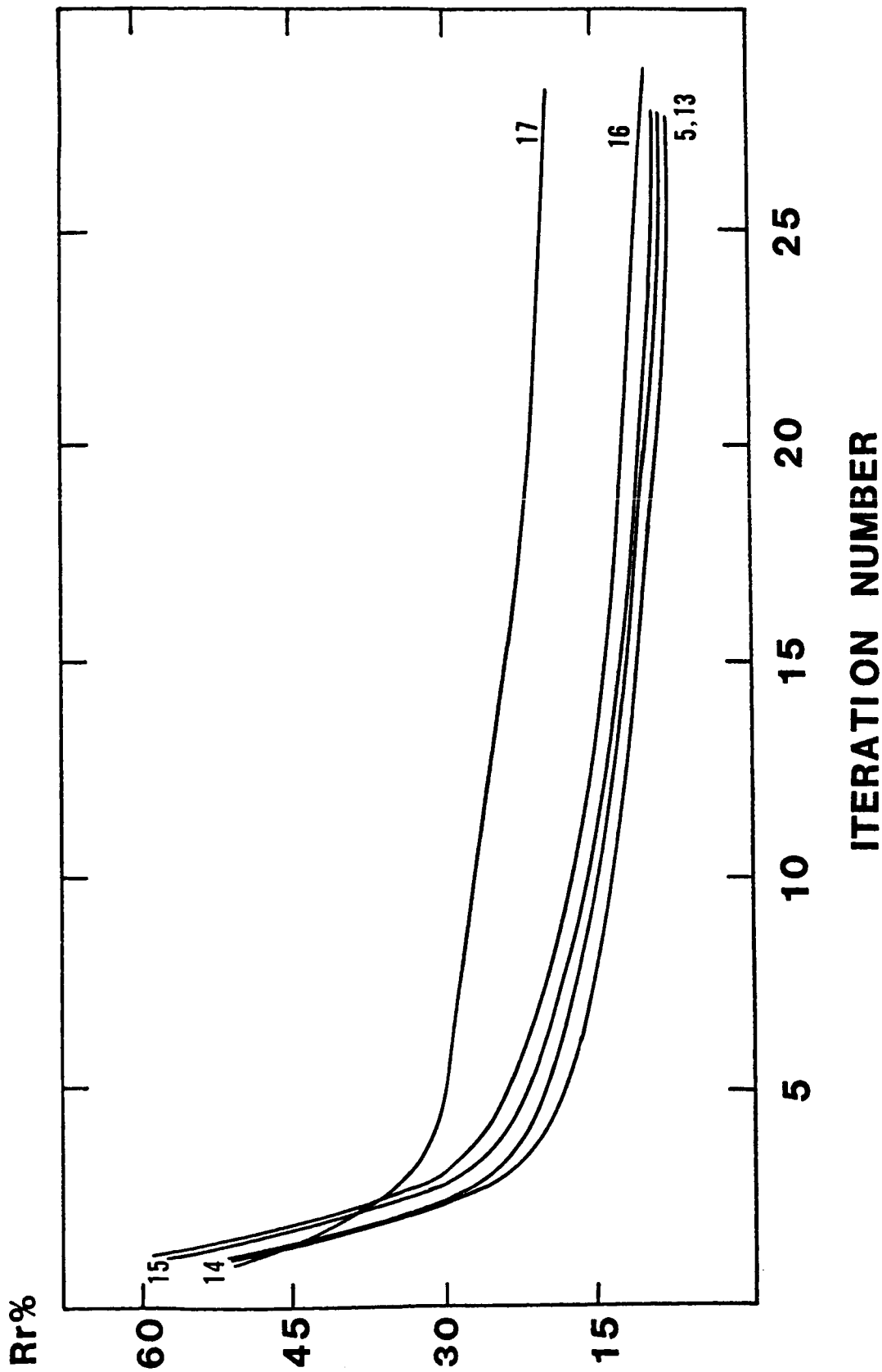

Figure 6. Inversion errors vs. iteration number for different view angles (fringe number round-off error = 0.05 λ).

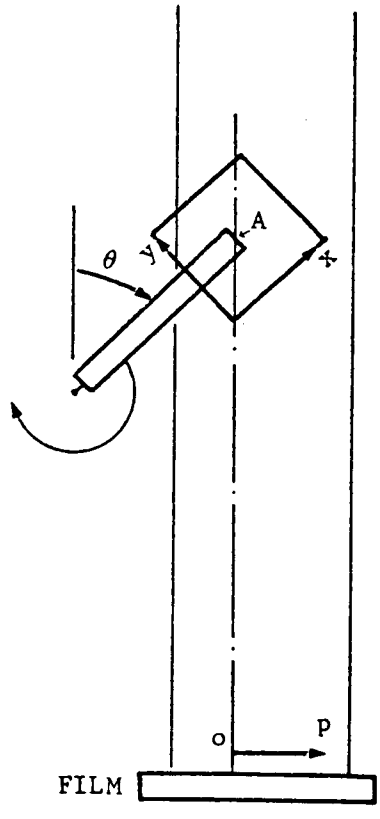

Figure 7. Rotating blade tip region and the coordinates.

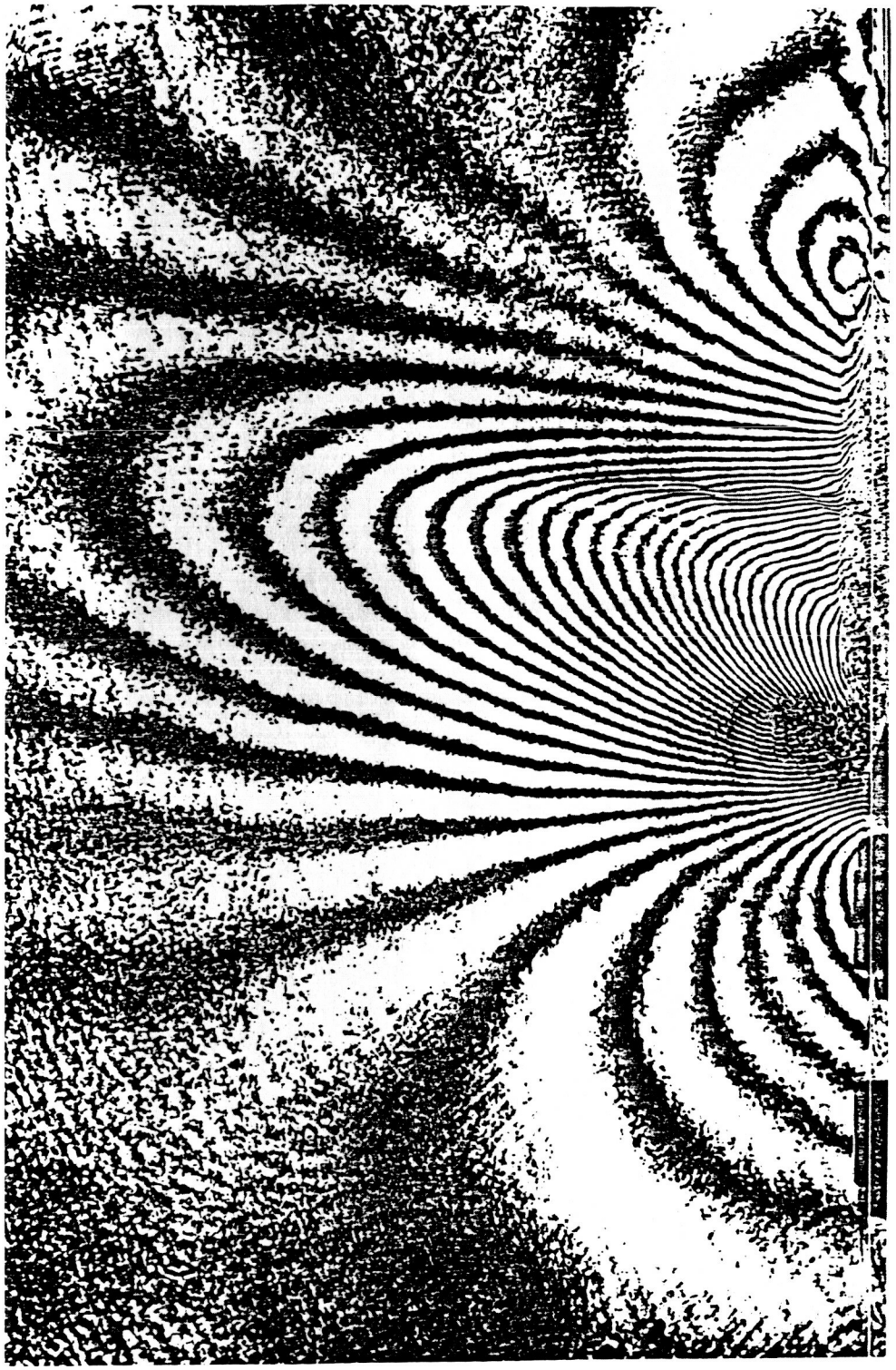

Figure 8. Interferogram of flow over a rotating blade, $\theta = 176.5°$.

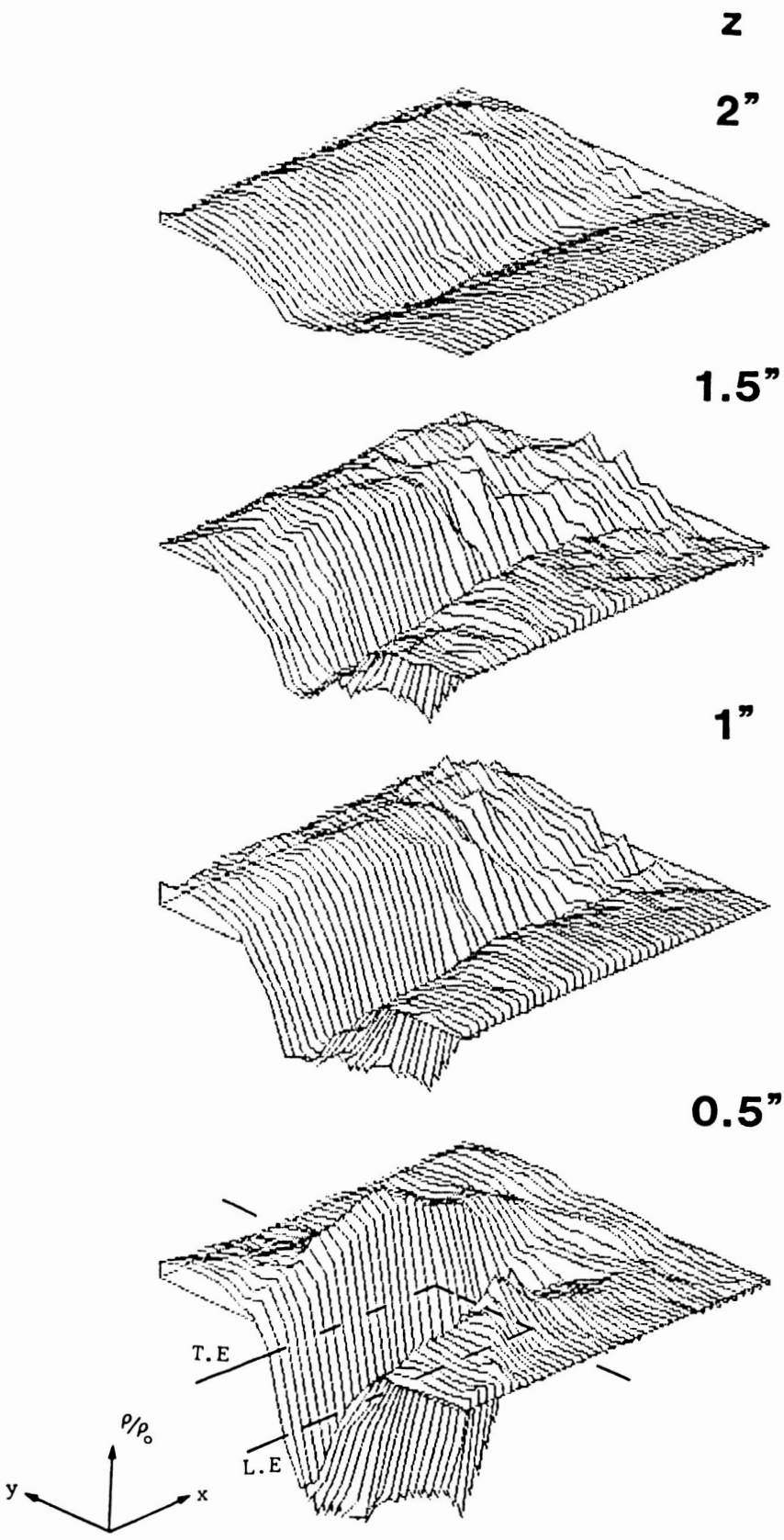

Figure 9. Reconstructed density fields for different heights above blade chord line.

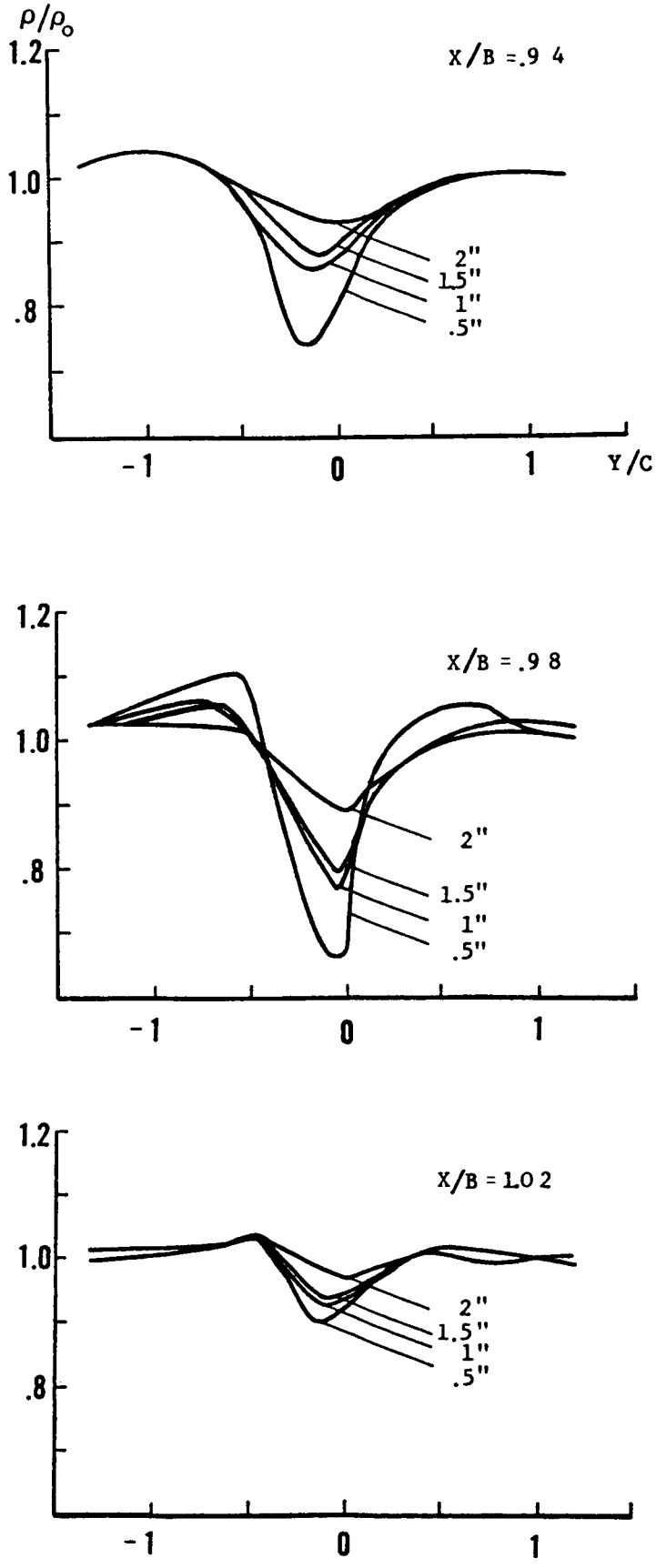

Figure 10. Density ratio profiles (blade length B = 41.1", chord length C = 3").